Ocean Sci. Discuss., 11, 425–452, 2014
www.ocean-sci-discuss.net/11/425/2014/
doi:10.5194/osd-11-425-2014

Ocean Science
Discussions
Open Access

Extreme winter 2012 in the Adriatic: an example of climatic effect on the BiOS rhythm

M. Gačić, G. Civitarese, V. Kovačević, L. Ursella, M. Bensi, M. Menna, V. Cardin, P.-M. Poulain, S. Cosoli, G. Notarstefano, and C. Pizzi

OGS (Istituto Nazionale di Oceanografia e di Geofisica Sperimentale), Trieste, Italy

Received: 18 December 2013 – Accepted: 24 January 2014 – Published: 3 February 2014

Correspondence to: M. Gačić (mgacic@ogs.trieste.it)

Published by Copernicus Publications on behalf of the European Geosciences Union.

Abstract

Adriatic and Ionian Seas are Mediterranean sub-basins linked through the Bimodal Oscillating System mechanism responsible for decadal reversals of the Ionian basin-wide circulation. Altimetric maps showed that the last cyclonic mode started in 2011 but unexpectedly in 2012 reversed to anticyclone. We related this “premature” inversion to extremely strong winter in 2012, which caused the formation of very dense Adriatic waters, flooding Ionian flanks in May and inverting the bottom pressure gradient. Using Lagrangian float measurements, the linear regression between the sea surface height and three isopycnal depths suggests that the southward deep-layer flow coincided with the surface northward geostrophic current and the anti-cyclonic circulation regime. Density variations at depth in the north-western Ionian revealed the arrival of Adriatic dense waters in May and maximum density in September. Comparison between the sea level height in the north-western Ionian and in the basin centre showed that in coincidence with the arrival of the newly formed Adriatic dense waters the sea level lowered in the north-western flank inverting the surface pressure gradient. Toward the end of 2012, the density gradient between the basin flanks and its centre went to zero, coinciding with the weakening of the anticyclonic circulation and eventually with its return to the cyclonic pattern. Thus, the premature and transient reversal of Ionian surface circulation originated from the extremely harsh winter in the Adriatic, resulting in the formation and spreading of highly dense bottom waters. The present study highlights the remarkable sensitiveness of the Adriatic–Ionian BiOS to climatic forcing.

1 Introduction

Thermohaline circulation (THC) is a part of the Meridional Overturning Circulation (MOC), the total northward/southward flow in the World Ocean. In driving the thermohaline component of the MOC, salinity presumably has a limited effect with respect to the temperature (Rahmsdorf, 2006). The Mediterranean Sea (MS) has been considered as a laboratory basin for some processes and circulation features occurring in the World Ocean (Bethoux et al., 1990).

Contrary to the THC where differences in the heat content play a major role, the salinity contrast between the inflowing Atlantic Water (AW) and the Levantine surface and intermediate waters (Robinson et al., 2001) drives and largely maintains the Mediterranean basin-wide circulation. The high salinity waters originating in the Levantine and, in general, in the Eastern Mediterranean (EM) are related to the excess of evaporation over precipitation. The Mediterranean Overturning Circulation (MedOC), due to the east–west climatic differences, is zonally oriented contrary to the THC which is essentially a meridional flow. In addition, in the World Ocean the entire or a larger part of the water column is affected by the north/south flows. In contrast, the MedOC is limited to the surface and intermediate layers due to two factors: the first one is that the Levantine Intermediate Water (LIW) in the EM is not dense enough to sink to larger depths and thus spreads in the intermediate layer (~ 300 m); the second factor is the bathymetry in the Sicily and Gibraltar Straits (with depths < 500 m). In addition to the thermohaline forcing, the wind-driven circulation represents an important component of the MedOC. Winds are highly variable on seasonal and interannual scales as well as spatially and thus their influence on MedOC is not fully quantified. Generally, from available wind data, it was shown that in the northern portion of the Mediterranean the wind curl is prevalently cyclonic while in its southern part is anticyclonic imparting positive and negative vorticity to the oceanic flow, respectively (Pinardi et al., 2013).

In contrast to the world ocean where vertical convection makes an integral part of the MOC, in the MS the ventilation of the deep portion of the water column only partially interacts with the MedOC (Lascaratos et al., 1999). The winter convection and deep water formation taking place in the northern parts of the MS, i.e. in the Gulf of Lion in the WM and in the Adriatic/Aegean in the EM, make part of the closed meridional thermally-driven circulation cells. The coupling with the MedOC is achieved via LIW whose presence in the dense water formation sites (Gulf of Lion and Adriatic/Aegean Sea) represents a key ingredient in facilitating the vertical convection and in determining the thermohaline properties of the deep water formed. Therefore, in the MS two types of circulation cells co-exist: the zonal MedOC, driven mainly by the east-west salinity gradient interacting with two secondary cells controlled by the north-south temperature gradient, where the driving mechanisms are the winter air–sea heat losses and vertical convection.

As opposed to the world ocean, decadal variability of the MedOC is rather well assessed. The idea of the Mediterranean circulation being in a steady state was definitely abandoned when in the early 1990's the Eastern Mediterranean Transient (EMT) was discovered. The phenomenon manifested essentially in the Aegean/Cretan Sea substituting the southern Adriatic as the dense water formation site (Roether et al., 1996). This abrupt change was attributed in a number of numerical studies to a meteorological forcing (Beuvier et al., 2010) and to the Levantine circulation changes bringing highly saline waters into the Cretan Sea. Salinity increase in the Levantine was also explained in some experimental studies in terms of a blocking of the LIW outflow through the Cretan Passage (Malanotte-Rizzoli et al., 1999). Subsequently, deep winter convection and bottom water formation in the Cretan Sea took place following severe winter climatic conditions.

Recently, cyclical occurrences of the high salinity in the Levantine and the EMT preconditioning have been explained in terms of the feedback mechanism called Adriatic–Ionian Bimodal Oscillating System (BiOS), i.e. the decadal reversals of the Ionian upper-layer basin-wide circulation from cyclonic to anticyclonic and vice versa (Gačić et al., 2011). The Mid-Ionian Jet, which brings AW into the Levantine basin, is reinforced or weakened by the Ionian cyclonic or anticyclonic circulation, respectively. This then results in a varying intensity of the AW advection towards the Levantine and consequently in a varying dilution of the Levantine surface waters. Considering that the LIW is formed in the Levantine, in the area of Rhodes Gyre, obviously the LIW salinity will change as a function of the intensity of the Levantine surface water dilution by the AW.

OSD
11, 425–452, 2014

During the Ionian anticyclonic mode the AW flow is mainly deflected northeastward affecting the northern Ionian and southern Adriatic. In that situation the flow of the AW towards the Levantine is reduced, the Levantine surface waters become saltier and the same applies to the LIW. The Ionian anticyclonic circulation mode is thus the preconditioning factor for the EMT-like phenomena (Gačić et al., 2011). Possible occurrence of the EMT would then take place only if the air–sea heat losses in the Aegean are strong enough to produce deep convection.

The Adriatic Sea as a dense water formation site is more prone to winter convection when the Ionian circulation is cyclonic bringing there the salty waters of the Levantine origin. In the opposite circulation pattern, under the influence of the AW, the vertical stability of the water column in the Adriatic hampers the vertical convection. In addition, the water formed is of a lower salinity due to the freshening of the upper part of the Adriatic water column. From these considerations, one can explain why the Levantine and Adriatic salinities are out of phase and why the Aegean and Adriatic were substituting each other as a source of the Eastern Mediterranean Deep Water (EMDW) during the EMT. However, we have to take into considerations that the winter convection in the Adriatic depends on the interplay between air–sea heat fluxes and the buoyancy content and thus winter meteorological conditions can modify the efficiency of the Adriatic as a source of the EMDW. In addition to the variability of the efficiency of the Adriatic dense water source as a function of the buoyancy content, the density of the Adriatic Dense Water (AdDW) depends on the salinity of the inflowing water (Levantine or Atlantic origin).

From the historical T-S data in the last sixty years (Gačić et al., 2013) it was evidenced that e.g. the salinity minimum in the North Ionian, presumably associated with the anticyclonic phase of North Ionian Gyre (NIG) occurred cyclically on time scales between four and eleven years. This means that NIG inversions appear at the same time scales. From the altimetric data, the occurrences of two anticyclonic phases in the Ionian (1987–1997 and 2006–2010) have been identified. In addition, two cyclonic phases have been documented, the first one in the period 1998–2005, and the second one which started in 2011. However, in 2012 the unexpected reversal from the cyclonic to the anticyclonic mode took place. The aim of this study is to analyse this "premature" inversion of the NIG trying to explain it in terms of the extremely severe climatic conditions in the Adriatic during the winter 2012, thus relating it to the spreading of the very cold and dense AdDW formed during that winter.

2 Data and methods

A fleet of 17 Argo profiling floats is used for this work. They operated between 2011 and 2012 in the Ionian Sea. They were deployed in the framework of the Argo program in the Mediterranean Sea (MedArgo, see Poulain et al., 2007). The profilers were equipped with Sea-Bird CTD (Conductivity-Temperature-Depth) sensors (models SBE 41 or 41CP) with accuracies of ±0.002 °C, ±0.005 and ±2.4 dbar for temperature (T), salinity (S), and pressure (P), respectively. The sampling depth was variable: in the upper layer, it is set to 5 dbar in the interval [0,100]; 10 dbar in the interval [100,700], 50 dbar in the interval [700,2000], including the near bottom values. Some notoriously spurious values were eliminated. The Argo floats were programmed with a cycle length between 2 and 10 days, a drifting depth of 350 or 1000 m and a maximal profiling depth between 1000 and 2000 m. The data were processed and quality-controlled using a basic set of tests at the Argo Data Assembly Centre (DAC). A delayed-mode quality control of P, T and S data was then applied in accordance to the Argo Quality Control Manual (2013), Version 2.8, 3 January 2013, Argo Data Management (available at http://www.argodatamgt.org/content/download/15699/102401/file/argo-quality-control-manual-version2.8.pdf) and in particular the Owens-Wong method was adopted (Owens and Wong, 2009) to check the S data. The Argo float S profiles were also qualitatively compared to a reference dataset (see details in Notarstefano and Poulain, 2008); this comparison detected no drift of the conductivity sensor for the majority of the floats. A significant negative offset (0.0151 PSU) in the S data was evidenced only for Argo float 6900952 (Notarstefano and Poulain, 2013),

OSD
11, 425–452, 2014

which was later corrected. After removing the spikes, the potential drifts or offsets of the T and conductivity sensors were detected to be smaller than the natural variability of the water column and hence no delayed mode correction was deemed necessary.

The altimetry data used for this study are gridded (1/8° Mercator projection grid) Ssalto/Duacs weekly, multi-mission, delayed time (quality controlled) products from AVISO (SSALTO/DUACS users handbook 2013). Among the available versions of the delayed time products we have selected the reference data series, based on two satellite (Jason-2/Envisat or Jason-1/Envisat or Topex/Poseidon/ERS) with the same groundtrack. These data series were homogeneous all along the available time span, thanks to a stable sampling. Absolute dynamic topography (ADT) and corresponding absolute geostrophic velocities (AGV) data were downloaded. The ADT is the sum of sea level anomaly and Synthetic Mean Dynamic Topography, estimated by Rio et al. (2007) over the 1993–1999 period.

Annual and monthly averages of the ADT and AGV in the Ionian Sea were estimated over the 2008–2012 period. The AGV were sub-sampled in non-overlapping bins of 0.25° × 0.25°. Time-series of the weekly spatially averaged zonal geostrophic components were calculated in an area of the Northern Ionian (see Fig. 1).

Vertical profiles of horizontal geostrophic currents were derived at discrete depth levels by vertically integrating the thermal-wind equation. Interpolated (1 m vertical resolution) vertical profiles of potential density were derived from the available T-S profiles for the period June–November 2012. The required horizontal gradients of potential density were derived by locally fitting horizontal density planes to each grid point using density measurements from nearby locations. The 350 m level, where float-derived velocity field was available, was chosen as reference level to obtain absolute velocity profiles. The absolute velocities were then compared with the surface geostrophic flow in order to assess the seasonal influence.

Air–sea heat fluxes were calculated at the air–sea interface every 6 h (00:00, 06:00, 12:00, 18:00 UTC) from the European Center for Medium Range Weather Forecast, Reading, UK (ECMWF) Operational Analysis Data Set using a 0.25° interpolated lat/lon

OSD
11, 425–452, 2014

Extreme winter 2012 in the Adriatic

M. Gačić et al.

Gaussian grid (Cardin and Gačić, 2003). From the 6 hourly values, instantaneous flux components for long-wave (May, 1986), sensible and latent heat flux (Kondo, 1975) were obtained. These were subsequently averaged to obtain daily mean values, while the short-wave radiation was determined as an integral from sunrise to sunset, according to Schiano (1996). Adding its value to the mean of the other three components, the daily net heat flux was determined at each grid node. More information on formulas applied and coefficients can be found in Cardin and Gačić (2003). Mean area winter heat losses were then calculated for the period spanning from 1 December to 31 March using a grid of 157 nodes for the Southern Adriatic basin for three consecutive winters i.e. 2009–2010, 2010–2011 and 2011–2012.

Correlation between the Absolute Dynamic Topography (ADT) and the depth of the isopycnals 29.00, 29.10 and 29.18 $kg\,m^{-3}$ obtained from in-situ conductivity-temperature-depth (CTD) casts were computed for the two periods June–November 2011 and June–November 2012. Correlation coefficients were calculated between the six-months average ADT values and isopycnal depths at each CTD position.

Due to the paucity of float data for the period June–November 2011, the float dataset were merged with CTD profiles coming from the POS414 cruise (R/V *Poseidon*), carried out in June 2011 in the Eastern Mediterranean (Tanhua et al., 2013). All profiles referred to the POS414 cruise were sampled using a CTD-rosette equipped with a SBE19plus sensor, with overall accuracies of ±0.002 °C, ±0.003 for temperature and salinity, respectively. Potential density anomalies (reference pressure equaling zero) were computed with MATLAB using TEOS-10 thermodynamic equations of seawater (http://www.teos-10.org/pubs/TEOS-10_Manual.pdf).

3 Data analysis and discussion

In order to illustrate decadal inversions of the Ionian basin-wide circulation for the last two decades, we present time-series (Fig. 2) of the zonal component of the surface

OSD
11, 425–452, 2014

geostrophic currents computed for the northern portion of the Ionian (see Fig. 1 for the position of the area where the average geostrophic currents were calculated). We present both low-pass monthly time-series filtered by the 13 month moving average and the complete signal. From the unfiltered time-series, clear seasonal variability emerged. Positive zonal geostrophic component (eastward) represents the anticyclonic circulation while the negative one is associated with the cyclonic Ionian mode. Generally, the zonal component of the geostrophic current varies primarily at the decadal time scale. The seasonal basin-wide circulation reversals occurred only in the transitional phase between the two subsequent decadal circulation patterns like in the late 1990's, around 2006 and around 2009. From the presented time-series there are evidences suggesting that the BiOS anti-cyclonic mode which started in late 1980's was of a longer duration than the anti-cyclonic phase starting in 2006. The same is very likely valid for the cyclonic modes. This could be explained in terms of the EMT, when much larger quantities of the Aegean dense waters (3 Sv average outflow between mid-1992 and late 1994 according to Roether et al., 2007) than the "normal" AdDW volume (0.3 Sv – Lascaratos, 1993) flooded the Ionian abyssal area. We will be analysing the mechanism potentially responsible for the unexpected reversal, which took place in 2012 and clearly documented from both monthly and yearly altimetric maps, presented here (Fig. 3). Altimetric data and surface geostrophic currents (annual mean maps) from 2008 to 2012 show the second part of the anticyclonic phase in the late 2000's and the breaking up of the basin-wide anticyclonic meander into several mesoscale cyclonic and anticyclonic features. The complete reversal from the anticyclonic to the cyclonic mode took place in 2011 (Fig. 3d) when the large cyclonic area occupied the Northern Ionian. Subsequently, the new "premature" reversal from the cyclonic to anticyclonic circulation took place in 2012 (Fig. 3e), when the northward protrusion of the anticyclonic meander was evident. From the monthly mean altimetric maps for 2012 (Fig. 4), we can identify with more precision the reversal time. It is evident that the reversal of the NIG from cyclonic to anticyclonic initiated with the break-up of the sub-basin scale cyclone into two mesoscale cyclones in May 2012. Between these

OSD
11, 425–452, 2014

two cyclones, the establishing and strengthening of the anticyclonic meander became more and more evident protruding northward. This latter circulation pattern reached its maximum in the period August–November.

In December, the anticyclonic meander started to withdraw leaving again room to the cyclonic circulation and very likely to an eventual re-establishment of the cyclonic BiOS phase which is evident in the altimetric maps for January, February and March 2013. To a certain extent, this change of pattern can be associated to intra-annual variability but as shown, the seasonal signal very rarely can invert the basin-wide circulation.

We will now try to explain the "premature" Ionian basin-wide circulation reversal occurring in the period May–November in terms of effect of the cold and dense AdDW formed during the extremely cold 2012 winter. According to recent papers (Bensi et al., 2013; Mihanović et al., 2013; Vilibić et al., 2013) the winter 2012 was very harsh in the northern Adriatic resulting in the formation of extremely dense bottom water in the shelf area. Density anomaly recorded in the northernmost end of the Adriatic attained 30.59 $\mathrm{kg\,m^{-3}}$, the value reached only twice in the last 100 yr. Mihanović et al. (2013) showed that the average annual transport of the Northern Adriatic dense water reached a value, which was approximately a half of the average dense water formation rate in the southern Adriatic. Therefore, a contribution of the northern Adriatic dense water to the total volume of the AdDW was probably much larger than about 10 % as estimated by Vilibić and Orlić (2002). Apart from the effect of the northern Adriatic dense water on the outflowing AdDW, the heat fluxes in the open-ocean convection area in the southern Adriatic were also very strong. More precisely, the comparison of the surface heat losses between three consecutive (2010, 2011 and 2012) winters (December–March period) for the southern Adriatic confirmed that they were strongest in winter 2012. Six episodes with the surface heat losses stronger than 400 $\mathrm{W\,m^{-2}}$ occurred in January–February of 2012, while in other two years such episodes were practically absent (Fig. 5). Subsequently, cold and very dense water formed locally in the Southern Adriatic with an important contribution of the Northern Adriatic dense water spread along the western flank of the Ionian. It generated the pressure gradient force oriented

OSD
11, 425–452, 2014

from the coast toward the open sea, and consequently the deeper-layer southward geostrophic flow. Due to the presence of the dense water along the western Ionian flank, the sea level along borders became lower than in the centre. Therefore, the southward motion of the colder and denser Adriatic water along the western Ionian flanks generated the northward surface geostrophic flow. This is a qualitative explanation of the "premature" reversal of the NIG associated with the spreading of the very cold and dense Adriatic waters.

In order to compare the sea level structure and the isopycnal depth, we calculated the linear correlation between the altimetric data and the isopycnal depths for 2011 and 2012 (Fig. 6). If such a relation exists, it would mean that the Ionian behaved as a two-layer basin, i.e. that the upper-layer cyclonic or anticyclonic flow was in the opposite direction with respect to a deep layer circulation as hypothesized earlier in this paper. In other words, this would suggest that the surface geostrophic circulation was related to the deeper layer flow and that the sea level pattern was representative of the horizontal distribution of isopycnal depths. We have chosen 29.00, 29.10 and 29.18 $\mathrm{kg\,m^{-3}}$ isopycnal depths for the comparison with the sea surface height. The average depth of the 29.00 $\mathrm{kg\,m^{-3}}$ isopycnal was about 200 m; the 29.10 $\mathrm{kg\,m^{-3}}$ isopycnal corresponds to the LIW and occupied depths of around 300 m. The 29.18 $\mathrm{kg\,m^{-3}}$ isopycnal can be considered as the lower limit of the AdDW density in the Ionian located around 1100 m depth. We have compared semi-annual mean sea level data (June–November) with the isopycnal depth at a given point obtained from the floats. We have chosen the 6 month period when spatially the most homogeneous float data coverage was present in both 2011 and 2012. In addition, we expect that in the chosen period June–November the newly formed AdDW very likely reached the Ionian. Considering all the float data within the 6 month period together means that we hypothesized small intra-annual variations in the density field. This was a reasonable assumption for the portion of the water column below the seasonal pycnocline. However, some noise over the entire depth range may derive from the mesoscale variability affecting float trajectories. In 2012, the regression was close to linear for the first two isopycnals with the decreasing values of the

OSD
11, 425–452, 2014

correlation coefficient with depth. On the other hand, the data points in the sea level $-29.18\,\mathrm{kg\,m^{-3}}$ isopycnal diagram were highly dispersed. During 2011 the float data coverage in the Ionian was poorer than in 2012 (Fig. 1) and thus we combined data from the oceanographic campaign carried out in June by R/V *Poseidon* and the float data. In the upper part of the water column (isopycnals 29.00 and $29.10\,\mathrm{kg\,m^{-3}}$) there were no important differences between 2011 and 2012 in the relationship between the isopycnal depth and the free surface; both years showed a statistically significant linear correlation. The $29.18\,\mathrm{kg\,m^{-3}}$ isopycnal depth showed higher correlation with the free surface for 2011 than for 2012. This difference can be explained by the fact that the spreading of the very dense AdDW in 2012 introduced spatial heterogeneity in the density field in the deeper part of the water column, which then resulted in the poor correlation between the free surface and the $29.18\,\mathrm{kg\,m^{-3}}$ isopycnal depth. In fact, as we will show later, a current reversal took place somewhere below the 750 m depth probably close to the depth of $29.18\,\mathrm{kg\,m^{-3}}$ and this could explain the lack of correlation. The statistically significant correlation confirmed the interdependence of the surface and deeper layer circulation showing that from the surface geostrophic current pattern it is possible to reconstruct the deeper layer flow. In the specific case of 2012, the massive inflow of the dense AdDW generated the reversal of the Ionian surface circulation which, as shown from the linear regression between the sea surface height and isopycnal depth, was concomitant with the deeper layer circulation inversion. It is also important to stress that data points, independently on the float and its position were scattered along the same straight line.

Next, we will analyse in more details the temporal variations of the water density from the float measurements. We looked for evidences on the evolution of the horizontal density gradient in the deeper portion of the water column between the centre of the Ionian and its flanks, which resulted in a reversal of the surface pressure gradients and of the geostrophic flow. We will estimate the timing of the change of the horizontal density gradient due to the spreading of the highly dense AdDW and compare it with the sea level gradient reversal. The series of profiles (Fig. 7) revealed the density increase in the north-western Ionian starting in June related to the arrival of the newly formed AdDW. Thus, we should expect that the reversal of the density and surface pressure gradients first took place in that area. The temporal evolution of the average density in the deep portion of the profile (1000–1200 m layer) obtained from floats in the centre of the basin was compared with the density variations along the Ionian western flanks. For that purpose, we used data from two floats, which were mainly moving near the flanks, i.e. one in the northern part just downstream of the Strait of Otranto and the other one further southward along the Calabrian coast (Fig. 8a). Then the density data were compared with those in the centre of the basin obtained from one float whose motion was mainly limited to the central area of the Ionian representative of the density variations in the basin interior. The prominent density increase in the north-western Ionian occurred in the period from May through September reaching its maximum in August, period when presumably high-density AdDW was spreading along the north-western Ionian flanks as revealed from the density profiles. The density in the centre of the basin remained invariate thus during the AdDW spreading period a building up of a density gradient between the basin flank and its centre was taking place. Subsequently, the signal of the relatively high density reached the Calabrian coast around November (Fig. 8b), i.e. with an average speed of about 5 $cm\,s^{-1}$. It was rather weak probably because we compared the average density in the layer 1000–1200 m for all three sets of data. At the beginning of its spreading in the Ionian, the AdDW occupied mainly the layer around the 1000 m depth and thus the signal was very strong. This was particularly evident from the density profiles at the float positions indicated by the triangle and the cross in Fig. 7, which were located on the seaward side of the 1000 m isobath. The dense water in the interval of about ten days (29 July–9 August) deepened by about 300 m. Due to the deepening further downstream the AdDW presence was not so evident in the layer between 1000–1200 m. Together with the curve showing the evolution of the average density, we presented the sea level differences between the north-western area centred at the location where the AdDW signal in the density field was strongly present (as evidenced from the float profiles, see Fig. 7) and

OSD
11, 425–452, 2014

the centre of the basin. This comparison was done in order to reveal whether the sea level gradient and the surface geostrophic circulation reversals were concomitant with the density increase due to the arrival of the dense Adriatic waters. We considered the sea level differences between the centre of the basin and its north-western part instead of the geostrophic current in order to minimize the seasonal variability due to heating and cooling. On the other hand, the noise related to the presence of mesoscale eddies was very pronounced. Thus, we apply a low-pass filter to the time-series of the weekly sea-level differences. The low-pass curve of the sea-level differences showed clearly the lowering of the sea level in the north-western area with respect to the central zone of the Ionian basin related to the increase of the 1000–1200 m average density starting in May 2012. The sea level differences remained negative i.e. the sea level along the basin boundaries remained lower than in the centre until the beginning of 2013 although the vertically averaged density after September reached the same values as those at the open sea. This can be explained by the fact that the float in September left the area affected by the AdDW (see Fig. 8a) and thus reached the zone having densities rather close to those of the centre of the Ionian.

Further, in order to investigate the vertical flow structure and obtain the boundary between the upper and lower layer, we estimated the absolute current field. We computed the geostrophic shear from the float density field and added it to the measured Lagrangian velocity at the 350 m parking depth of the ARGO floats. We thus reconstructed the absolute velocity profile from the surface to the 750 m depth (Fig. 9). As far as the differences between the surface geostrophic flow and absolute currents are concerned, discrepancies at some locations were large but this can be explained in terms of the large interval we choose for the data analysis (June–November) when seasonal variability in the surface layer could be rather important. From Fig. 9 it is evident that the entire water column from the surface to the 750 m behaved mainly as a single layer meaning that the inversion took place below that depth. Only at one location, which was positioned in the north-western part of the basin and probably invaded by the AdDW, the two-layer structure was evident with the velocity at 750 m being in the

OSD
11, 425–452, 2014

opposite direction with respect to the surface one. Due to the scarcity of data, their uneven spatial distribution and the method for the horizontal density gradient calculations we were not able to cover in a more detailed manner the area in the close vicinity of the coast where we could expect the increased horizontal density gradients and large values of the vertical shear due to the presence of the AdDW. Another feature arising from the geostrophic shear calculations is that mesoscale structures (like e.g. large anticyclonic gyre in the centre of the Ionian) at the open sea were rather deep extending from the surface up to at least 750 m depth.

4 Conclusions

Here we documented from altimeter data that the NIG circulation, as a part of the BiOS decadal variability, passed from the anticyclonic circulation to the basin-wide cyclonic mode in 2011. This passage made part of the "regular" decadal inversions of the Ionian basin-wide circulation. In 2012, however unexpectedly the NIG became anticyclonic interrupting the most recent cyclonic BiOS phase. We showed that the winter 2012 in the southern Adriatic was extremely severe as already evidenced in the literature for its northern part and looked for the possible link between strong air–sea heat losses and the Ionian circulation inversion. We set up a hypothesis that extreme winter air–sea heat losses in both northern and southern Adriatic resulting in the formation of the cold and highly dense Adriatic bottom waters, spreading in the Ionian, inverted the bottom pressure gradient and generated the NIG reversal. We showed first that the sea level anomalies were linearly related to the depth of the three chosen isopycnals (29.0, 29.10, 29.18 kg m^{-3}) which confirmed that the Ionian behaved as a two-layer fluid. From the profiling floats, we also presented evidences on the temporal evolution of the spreading of the extremely dense Adriatic waters along the north-western Ionian flanks showing that it started in May 2012 and affected the density field until September. This was also the period of the major horizontal density gradient between the basin interior where the density did not change, and its western flanks. Computations of the

OSD
11, 425–452, 2014
Extreme winter 2012 in the Adriatic
M. Gačić et al.

sea surface differences between the north Ionian flank and the basin interior, and implicitly the geostrophic velocity, confirmed that in concomitance with the arrival of the Adriatic dense waters, the seaward sea surface pressure gradient was set up. With the decrease of the horizontal deep density gradients towards the end of 2012 the surface geostrophic flow, as part of the anticyclonic NIG weakened. Finally, we documented from altimetric data that the NIG circulation returned to the cyclonic one at the beginning of the 2013. From the vertical geostrophic shear and the absolute geostrophic velocity we were not able to determine the basin-wide distribution of the no-motion level i.e. the boundary between the upper and lower layer, because the float data reached only the 750 m depth and the no-motion level was probably below that depth. There were however indications that near the north-western flank the no-motion level or the boundary between the upper and lower layers was situated at depth shallower than 750 m.

In summary, here we evidenced that the BiOS mechanism is highly sensitive to the climatic conditions, more specifically to the air–sea heat fluxes in the Adriatic dense water formation areas which can affect its cycle. In fact, we presented here supporting elements to the thesis raised by Mihanović et al. (2013) which sustained that future climate variability will have an important effect in changing the BiOS temporal scale due to projected increase of cold air outbreaks in the 21st century. This study also implicitly confirmed that the NIG reversal can be explained solely in terms of the variations of thermohaline properties of the AdDW not excluding completely the wind forcing whose role has been underlined in a series of papers like e.g. Pinardi et al. (2013) and references cited therein.

Acknowledgements. This research was supported by the Italian Ministry of Education, University and Research (MIUR) under the RITMARE (Ricerca ITaliana per il MARE), MedGES (Mediterranean Good Environmental Status) and Argo-Italy projects. We acknowledge also a partial support from the EU project PERSEUS.

OSD
11, 425–452, 2014

References

Bensi, M., Cardin, V., Rubino, A., Notarstefano, G., and Poulain, P. M.: Effects of winter convection on the deep layer of the Southern Adriatic Sea in 2012, J. Geophys. Res. Oceans, 118, 6064–6075, doi:10.1002/2013JC009432, 2013.

Bethoux, J., Gentili, P. B., Raunet, J., and Tailliez, D.: Warming trend in the western Mediterranean deep water, Nature, 347, 660–662, 1990.

Beuvier, J., Sevault, F., Herrmann, M., Kontoyiannis, H., Ludwig, W., Rixen, M., Stanev, E., Béranger, K., and Somot, S.: Modeling the Mediterranean Sea interannual variability during 1961–2000: focus on the Eastern Mediterranean Transient (EMT), J. Geophys. Res., 115, C08017, doi:10.1029/2009JC005950, 2010.

Cardin, V. and Gačić, M.: Long-term heat flux variability and winter convection in the Adriatic Sea, J. Geophys. Res., 108, 8103, doi:10.1029/2002JC001645, 2003.

Gačić, M., Civitarese, G., Eusebi Borzelli, G. L., Kovačević, V., Poulain, P.-M., Theocharis, A., Menna, M., Catucci, A., and Zarokanellos, N.: On the relationship between the decadal oscillations of the Northern Ionian Sea and the salinity distributions in the Eastern Mediterranean, J. Geophys. Res., 116, C12002, doi:10.1029/2011JC007280, 2011.

Gačić, M., Schroeder, K., Civitarese, G., Cosoli, S., Vetrano, A., and Eusebi Borzelli, G. L.: Salinity in the Sicily Channel corroborates the role of the Adriatic–Ionian Bimodal Oscillating System (BiOS) in shaping the decadal variability of the Mediterranean overturning circulation, Ocean Sci., 9, 83–90, doi:10.5194/os-9-83-2013, 2013.

Kondo, J.: Air–sea bulks transfer coefficients in adiabatic conditions, Bound.-Lay. Meteorol., 9, 91–112, 1975.

Lascaratos, A.: Estimation of intermediate and deep water formation rates in the Mediterranean Sea, Deep-Sea Res.-Pt. II, 40, 1327–1332, 1993.

Lascaratos, A., Roether, W., Nittis, K., and Klein, B.: Recent changes in deep water formation and spreading in the eastern Mediterranean Sea: a review, Prog. Oceanogr., 44, 5–36, 1999.

May, P. W.: A brief explanation of Mediterranean heat and momentum flux calculations, Norda Code 322, 1 pp., available from Naval Ocean Research and Development Activity, NTSL Station, MS 39529, 1986.

Malanotte-Rizzoli, P., Manca, B. B., Ribera d'Alcala, M., Theocharis, A., Brenner, S., Budillon, G., and Ozsoy, E.: The Eastern Mediterranean in the 80s and in the 90s: the big transition in the intermediate and deep circulations, Dynam. Atmos. Oceans, 29, 365–395, 1999.

OSD
11, 425–452, 2014

Mihanović, H., Vilibić, I., Carniel, S., Tudor, M., Russo, A., Bergamasco, A., Bubić, N., Ljubešić, Z., Viličić, D., Boldrin, A., Malačič, V., Celio, M., Comici, C., and Raicich, F.: Exceptional dense water formation on the Adriatic shelf in the winter of 2012, Ocean Sci., 9, 561–572, doi:10.5194/os-9-561-2013, 2013.

Notarstefano, G. and Poulain, P.-M.: Delayed mode quality control of Argo floats salinity data in the Tyrrhenian Sea, Rel 2008/125 OGA 43 SIRE, Trieste, Italy, 33 pp., 2008.

Notarstefano, G. and Poulain, P.-M.: Delayed mode quality control correction for a salinity offset of Argo float WMO 6900952 in the Mediterranean sea, 2013/35 Sez, OCE 18 MAOS 2013.

Owens, W. B. and Wong, A. P. S.: An improved calibration method for the drift of the conductivity sensor on autonomous CTD profiling floats by θ-S climatology, Deep-Sea Res.-Pt. I, 56, 450–457, 2009.

Pinardi, N., Zavatarelli, M., Adani, M., Coppini, G., Fratianni, C., Oddo, P., Simoncelli, S., Tonani, M., Lyubartsev, V., Dobricic, S., and Bonaduce, A.: Mediterranean Sea large-scale low-frequency ocean variability and water mass formation rates from 1987 to 2007: a retrospective analysis, Prog. Oceanogr., online first, doi:10.1016/j.pocean.2013.11.003, 2013.

Poulain, P.-M., Barbanti, R., Font, J., Cruzado, A., Millot, C., Gertman, I., Griffa, A., Molcard, A., Rupolo, V., Le Bras, S., and Petit de la Villeon, L.: MedArgo: a drifting profiler program in the Mediterranean Sea, Ocean Sci., 3, 379–395, doi:10.5194/os-3-379-2007, 2007.

Rahmstorf, S.: Thermohaline Ocean Circulation, in: Encyclopedia of Quaternary Sciences, edited by: Elias, S. A., Elsevier, Amsterdam, 2006.

Rio, M.-H., Poulain, P.-M., Pascual, A., Mauri, E., Larnicol, G., and Santoleri, R.: A mean dynamic topography of the Mediterranean Sea computed from altimetric data, in-situ measurements and a general circulation model, J. Marine Syst., 65, 484–508, doi:10.1016/j.jmarsys.2005.02.006, 2007.

Robinson, A., Leslie, W., Theocharis, A., and Lascaratos, A.: Mediterranean Sea circulation, in: Encyclopedia of Ocean Sciences, vol. 3, Elsevier, New York, 1689–1705, 2001.

Roether, W., Manca, B. B., Klein, B., Bregant, D., Georgopoulos, D., Beitzel, V., Kovačević, V., and Luchetta, A.: Recent changes in the Eastern Mediterranean deep water, Science, 271, 333–335, 1996.

Roether, W., Klein, B., Manca, B. B., Theocharis, A., and Kioroglou, S.: Transient Eastern Mediterranean deep waters in response to the massive dense-water output of the Aegean Sea in the 1990s, Prog. Oceanogr., 74, 540–571, 2007.

OSD
11, 425–452, 2014

Extreme winter 2012 in the Adriatic

M. Gačić et al.

Schiano, E.: Insolation over the western Mediterranean Sea: a comparison of direct measurements and Reed's formula, J. Geophys. Res., 101, 3831–3838, 1996.

Tanhua, T., Hainbucher, D., Schroeder, K., Cardin, V., Álvarez, M., and Civitarese, G.: The Mediterranean Sea system: a review and an introduction to the special issue, Ocean Sci., 9, 789–803, doi:10.5194/os-9-789-2013, 2013.

Vilibić, I., Šepić, J., and Proust, N.: Observational evidence of a weakening of thermohaline circulation in the Adriatic Sea, Clim. Res., 55, 217–225, doi:10.3354/cr01128, 2013.

OSD
11, 425–452, 2014

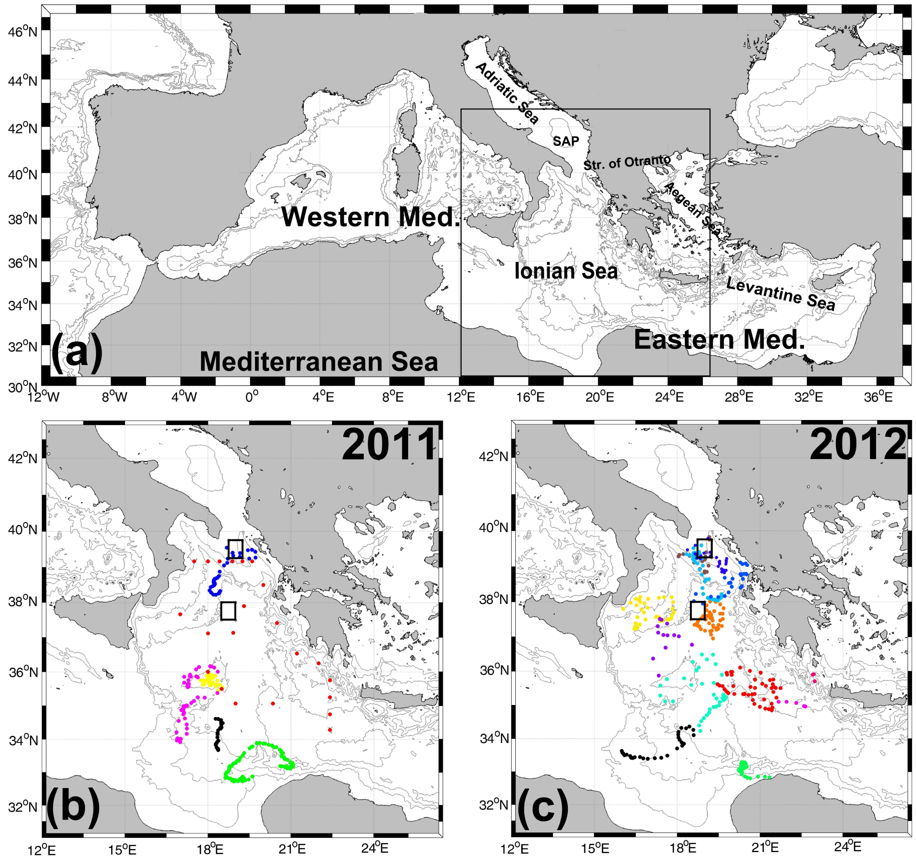

Fig. 1. Study area. Spatial distribution of the Argo float profiles; different colors represent different floats. Squares denote areas where the average sea level heights were calculated. The zonal component of the surface geostrophic flow was computed for the northern square.

OSD

11, 425–452, 2014

Extreme winter 2012 in the Adriatic

M. Gačić et al.

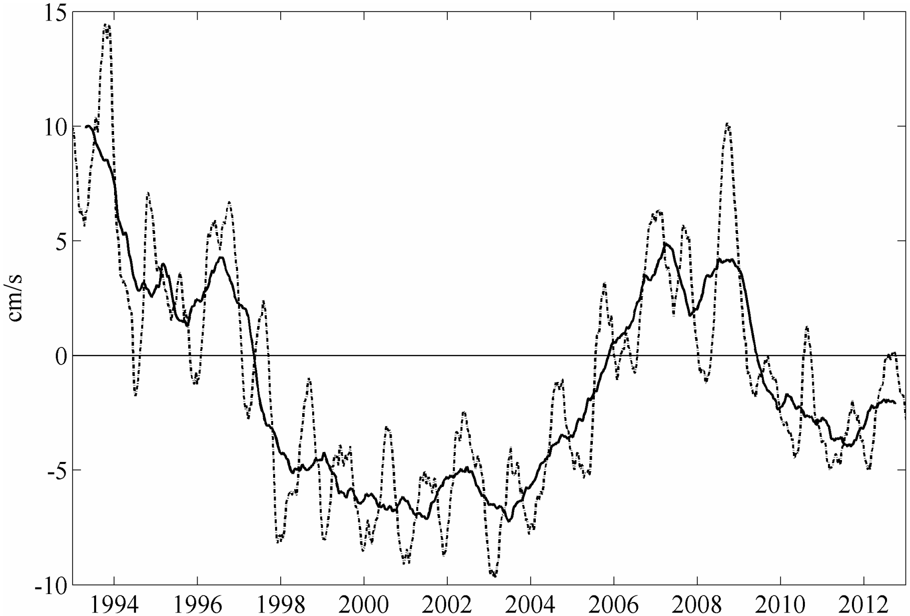

Fig. 2. Zonal component of the surface geostrophic velocity computed in the area denoted by the square (see Fig. 1). Continuous line represents the time-series smoothed by the 13 month moving average while the dashed line represents the total signal.

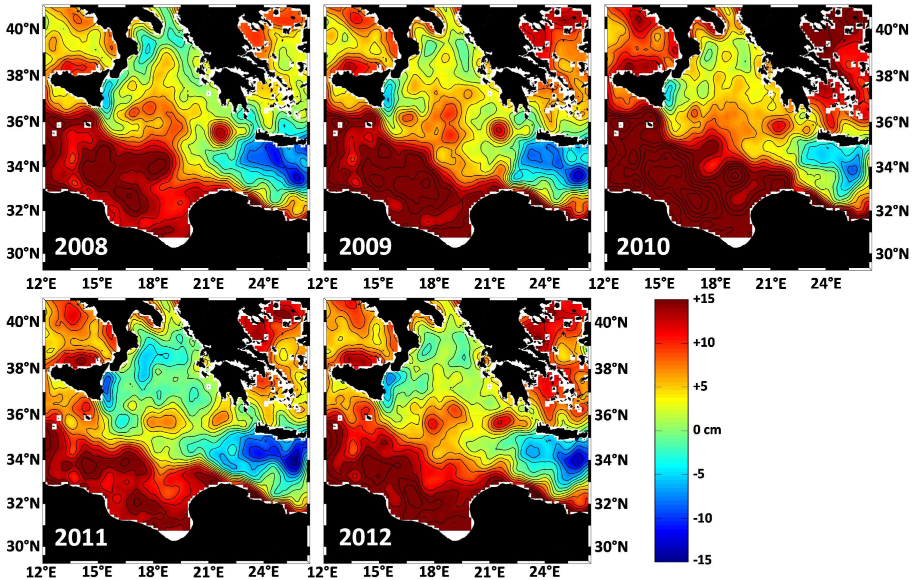

Fig. 3. Mean annual maps of the sea surface height for the period 2008–2012.

OSD
11, 425–452, 2014
Extreme winter 2012 in the Adriatic
M. Gačić et al.

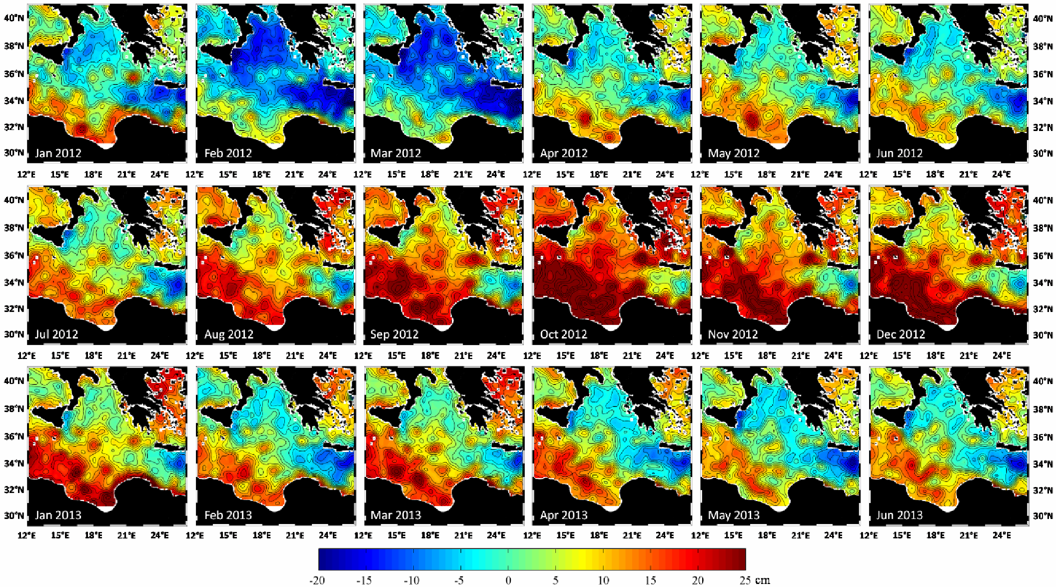

Fig. 4. Mean monthly altimetric maps for the period January 2012–June 2013.

OSD

11, 425–452, 2014

Title Page
Abstract | Introduction
Conclusions | References
Tables | Figures
◄| |►
◄ ►
Back | Close
Full Screen / Esc
Printer-friendly Version
Interactive Discussion

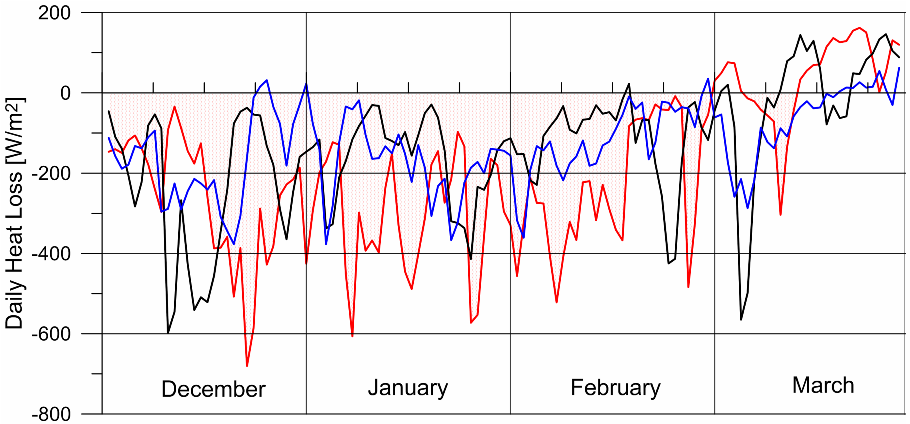

Fig. 5. Daily values of the surface air–sea heat fluxes for three consequtive winters (2010 – black line, 2011 – blue line and 2012 – red line).

OSD
11, 425–452, 2014

Extreme winter 2012 in the Adriatic

M. Gačić et al.

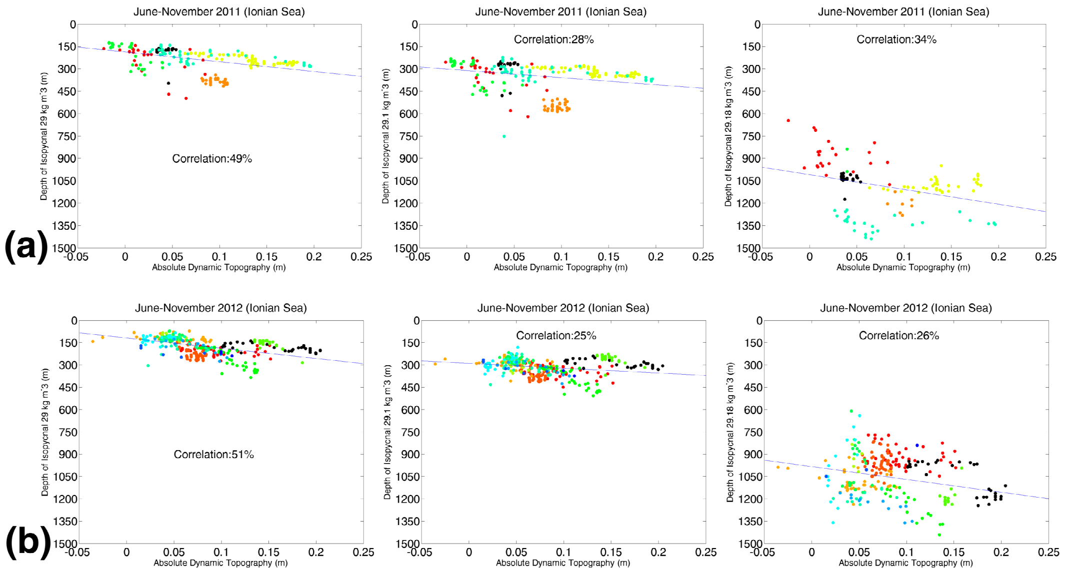

Fig. 6. Scatter plots of 29.0 (left), 29.05 (central) and 29.18 $kg\,m^{-3}$ isopycnal (right) depths vs. sea surface height. Color code of data points refer to different floats as evidenced in the Fig. 1.

OSD
11, 425–452, 2014

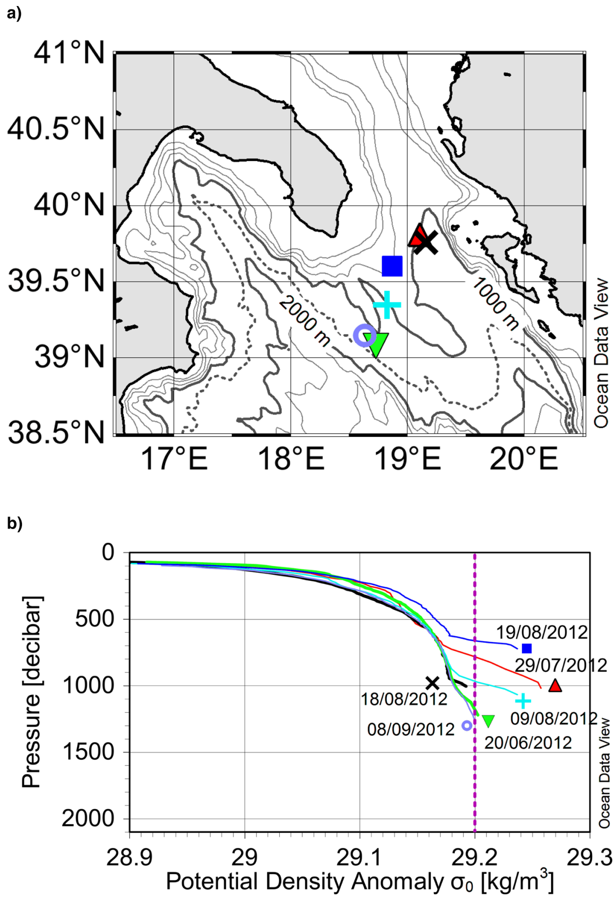

Fig. 7. Sampling locations of the profiling floats in the north-western Ionian area are presented on the map **(a)**, while the corresponding vertical density profiles are shown in **(b)**. The time of sampling is denoted next to the curves.

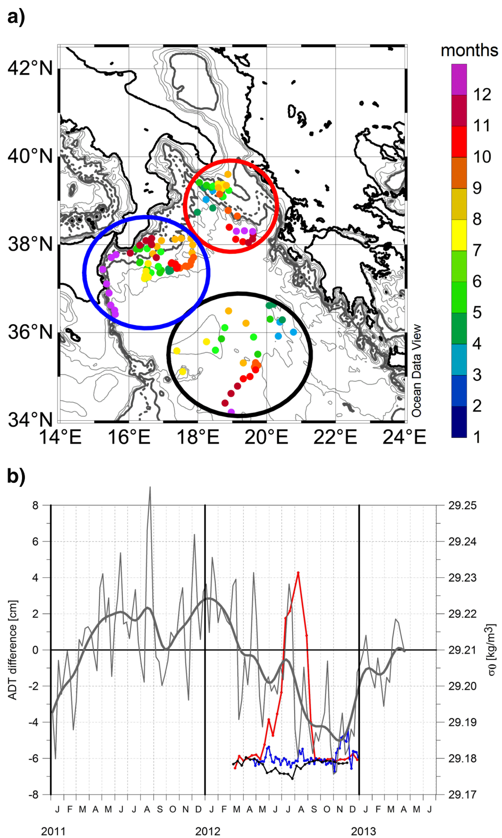

Fig. 8. Float sampling locations in the three areas **(a)** and the time series of the vertically averaged density within the depth interval 1000–1200 m (the colour of curves corresponds to the profile locations). The sea level differences computed between the two squares (northern square minus southern square, see Fig. 1 for the position of them) are also presented (bold line low-passed data, light line weekly data).

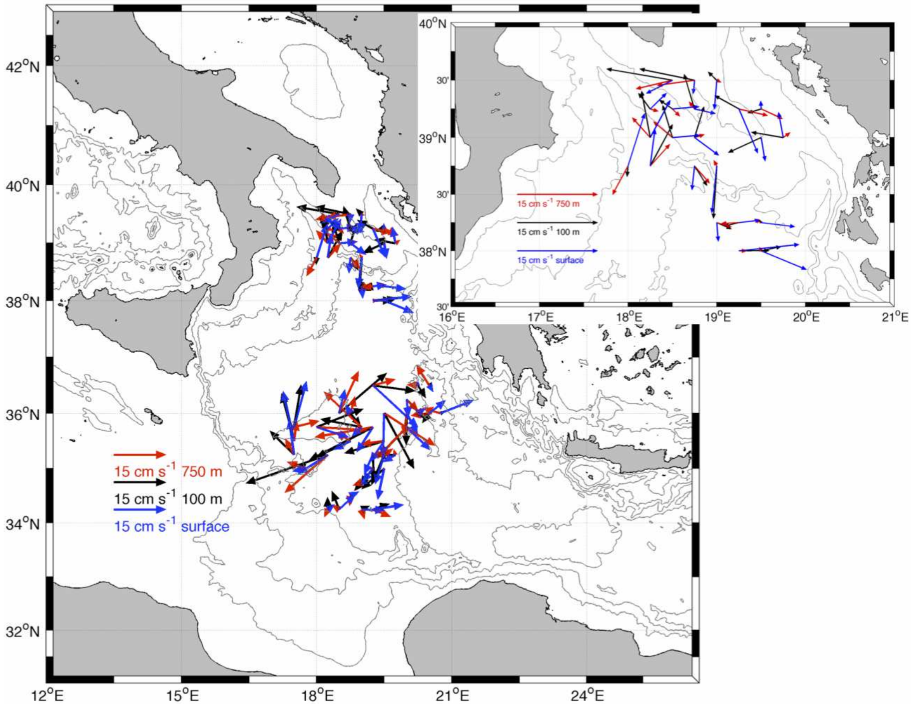

Fig. 9. Absolute velocities calculated from the geostrophic shear using the 350 m Lagrangian measurements as a reference velocity.

OSD
11, 425–452, 2014

Extreme winter 2012 in the Adriatic

M. Gačić et al.